IET Microwaves, Antennas & Propagation

Research Article

Hybrid technique for the analysis of circular waveguide junctions loaded with ferrite posts

ISSN 1751-8725
Received on 14th March 2014
Accepted on 29th November 2014
doi: 10.1049/iet-map.2014.0172
www.ietdl.org

Adam Kusiek ✉

Faculty of Electronics, Telecommunications and Informatics, Gdansk University of Technology, Poland
✉ *E-mail: adakus@eti.pg.gda.pl*

Abstract: This study presents a hybrid technique for the analysis of circular waveguide junctions loaded with axially symmetrical ferrite posts of irregular shape. The method is based on a combination of the finite-difference frequency-domain technique with a mode-matching technique. The proposed approach is validated by comparing the presented results with numerical ones obtained from commercial software. The application of a cylindrical junction loaded with ferrite posts with reciprocal and non-reciprocal devices is presented and discussed.

1 Introduction

Microwave devices utilising ferrite materials have been studied in the literature for decades [1–8]. Depending on the direction and spatial distribution of the biasing magnetic field it is possible to obtain different phenomena, such as field displacement [1, 2, 4–6], birefringence [7, 8] or Faraday rotation [3]. These effects are commonly utilised to design such non-reciprocal devices as circulators [1–4], isolators [5, 6] or phase shifters [7, 8].

The rigorous analytical solution of structures containing ferrite materials is limited to simple geometries for which the solution of wave equation can be determined [9–12]. Since, the analytical fields in ferrite posts have been known, they can be matched with the outer fields to calculate scattering parameters of waveguide structures or to determine the scattered field for open structures. In [12], utilising the solution in spherical coordinates, the radar cross-section of a configuration composed of concentric ferrite spheres was calculated. In [10, 13], the mode-matching (MM) technique was applied to determine the scattering parameters of circulator loaded with ferrite sphere and power divider loaded with ferrite cylinders, respectively.

In the case of structures containing ferrite posts with more complex geometry, the analytical solution is difficult or impossible to determine. Hence, the solution for such structures can be obtained by the more universal discrete techniques, for example, the finite-difference time-domain (FDTD) [14–16] or the finite element method (FEM) [17, 18]. The discrete techniques allow to take into account in the analysis the ferrite posts with arbitrary shape [14] and the direction of biasing magnetisation [16, 17]. However, in order to obtain sufficient accuracy of the results for complex structures, the high-density mesh has to be used, leading to long analysis time and high requirements for memory and CPU usage. In such cases hybrid techniques [19–21] combining analytical and discrete methods are more convenient. In this approach, discrete methods such as FEM or FDTD are utilised in the limited region where the analytical solution of the problem is difficult to determine. Next, the discrete solution is combined with analytically defined fields in the outer region. The advantages of this approach include higher versatility in comparison to analytical techniques [9–12] and lower numerical complexity in comparison to discrete techniques [14–18].

In this paper, a hybrid technique, previously presented in [22, 23], is developed for the analysis of circular waveguide structures containing an arbitrary configuration of ferrite posts. The proposed method is based on the combination of the finite-difference frequency-domain (FDFD) technique with the MM method. In my approach each object/configuration of objects is enclosed by an artificial sphere with boundary conditions defined by a transmission matrix [23]. The transmission matrix relates the incident field to the scattered field at the outer area of the artificial sphere, and is determined with the use of the finite-difference technique. Next, utilising the MM technique the discrete solution is combined with the analytical fields in the waveguide junction, resulting in scattering parameters of the structure. The advantage of assumed spherical representation of the object is the simplicity of matching fields defined on its surface with the fields coming from waveguide junction. Moreover, utilising additional theorem of spherical functions the transmission matrix of the configuration composed of arbitrary rotated and located objects can be easily derived. In order to speed up the analysis with the presented approach, we focus on axially magnetised and symmetrical ferrite posts. This allows us to reduce a three-dimensional (3D) problem to a two-and-a-half-dimensional one (2.5D). The convergence and validity of the approach are verified. The numerical results are compared with those obtained from commercial software and good agreement is observed.

2 Formulation of the problem

The investigated structure of waveguide junction is presented in Fig. 1.

The waveguide junction is loaded with axially symmetrical ferrite posts of irregular shape magnetised in a direction parallel to their axes of symmetry. In the analysis of the structure, the hybrid approach combining the FDFD technique with the MM technique is applied. In this approach, two main stages can be distinguished. First, each ferrite post in the structure is analysed separately with the use of the FDFD technique defined in a limited spherical region enclosing the object. As a result, the transmission matrix $\boldsymbol{T}$ relating an incident with scattered fields for each post/configuration in the structure is determined. Then, utilising the MM technique we match the fields from waveguide ports with the fields defined at the artificial spherical surfaces enclosing the investigated objects and as a result we obtain the scattering parameters of the junction. Section 2.1 presents the details of the scattering matrix calculation for the waveguide junction loaded with a spherical object represented by the transmission matrix. In Section 2.2, the outline of the $\boldsymbol{T}$-matrix calculation for configuration of arbitrary located and rotated ferrite objects with irregular shape is presented.

2.1 S-matrix

The investigated waveguide junction loaded with spherical object is presented in Fig. 2. In order to analyse the problem, the considered

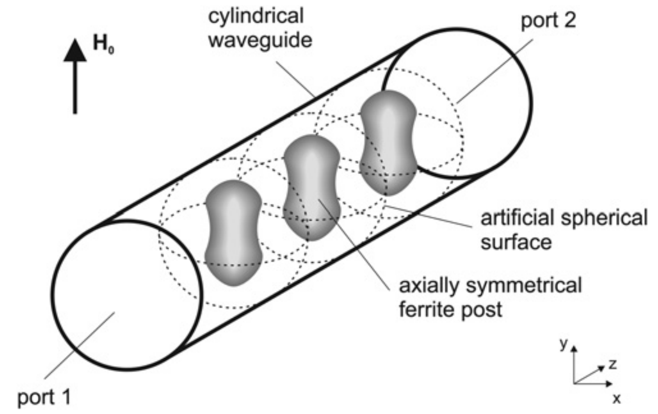

Fig. 1 *Investigated structure of waveguide junction loaded with ferrite posts*

structure is divided into two regions of investigations (see Fig. 2): region I, located inside the sphere of radius R, and region II, located outside this sphere in the cylindrical waveguide.

The longitudinal components of electric and magnetic fields in the ith waveguide junction port (region II) take the following form, suppressing $e^{j\omega t}$ time dependence [24]

$$E_z^{\mathrm{II},i} = \sum_{n=1}^{N_f} \sum_{m=-M}^{M} \frac{\left(p_{nm}^{\mathrm{TM},i}\right)^2}{\gamma_{nm}^{TM,i}} \left(t_{nm}^{\mathrm{TM},i} e^{-\gamma_{nm}^{\mathrm{TM},i} z} - r_{nm}^{\mathrm{TM},i} e^{\gamma_{nm}^{\mathrm{TM},i} z}\right) \psi_{nm}^{\mathrm{TM},i}(\rho, \varphi) \quad (1)$$

$$H_z^{\mathrm{II},i} = \sum_{n=1}^{N_f} \sum_{m=-M}^{M} \frac{\left(p_{nm}^{\mathrm{TE},i}\right)^2}{j\omega\mu} \left(t_{inm}^{\mathrm{TE},i} e^{-\gamma_{nm}^{\mathrm{TE},i} z} + r_{nm}^{\mathrm{TE},i} e^{\gamma_{nm}^{\mathrm{TE},i} z}\right) \psi_{nm}^{\mathrm{TE},i}(\rho, \varphi) \quad (2)$$

where $\gamma_{nm} = \sqrt{p_{nm}^2 - k_0^2}$ is the propagation coefficient along the z-axis, p_{nm} is the transverse wavenumber, $k_0 = \omega\sqrt{\mu_0 \varepsilon_0}$ is the wavenumber in free space, $\omega = 2\pi f_0$ and f_0 is the frequency of analysis. In above equations $\psi_{nm}(\rho, \varphi) = C_{nm} J_m(p_{nm}\rho) e^{jm\varphi}$, $J_m(\cdot)$ is the Bessel function of the mth order, C_{nm} are the normalisation coefficients defined as follows [24]

$$C_{nm}^{\mathrm{TM}} = \frac{\sqrt{2 - \delta_{m0}}}{p_{nm}^{\mathrm{TM}} R \sqrt{\pi} J'_m\left(p_{nm}^{\mathrm{TM}} R\right)}$$

$$C_{nm}^{\mathrm{TE}} = \frac{\sqrt{2 - \delta_{m0}}}{p_{nm}^{\mathrm{TE}} R \sqrt{\pi} \sqrt{1 - \left(m / p_{nm}^{\mathrm{TE}} R\right)^2} J_m\left(p_{nm}^{\mathrm{TE}} R\right)}$$

where δ_{m0} denotes the Kronecker delta and t_{nm}^i and r_{nm}^i are transmission and reflection coefficients in the ith waveguide port, respectively. Transverse components of electric and magnetic fields can be easily derived from Maxwell equations [24] utilising relations (1) and (2).

In region I, the total tangential to the surface $\mathcal{S}$ components of electric and magnetic fields are expressed as follows [25]

$$\boldsymbol{E}_t^I = \sum_{l=1}^{2} \sum_{n=1}^{N} \sum_{m=-n}^{n} \left\{ A_{lnm}^E z_n^l(k_0 r) \boldsymbol{M}_{nm}^t(\theta, \varphi) + A_{lnm}^H \frac{1}{k_0 r} \frac{\partial\left(r z_n^l(k_0 r)\right)}{\partial r} \boldsymbol{N}_{nm}^t(\theta, \varphi) \right\} \quad (3)$$

$$\boldsymbol{H}_t^I = \frac{j}{\eta_0} \sum_{l=1}^{2} \sum_{n=1}^{N} \sum_{m=-n}^{n} \left\{ A_{lnm}^H z_n^l(k_0 r) \boldsymbol{M}_{nm}^t(\theta, \varphi) + A_{lnm}^E \frac{1}{k_0 r} \frac{\partial\left(r z_n^l(k_0 r)\right)}{\partial r} \boldsymbol{N}_{nm}^t(\theta, \varphi) \right\} \quad (4)$$

where $\eta_0 = \sqrt{\mu_0 / \varepsilon_0}$, $z_n^1(\cdot)$ and $z_n^2(\cdot)$ denote spherical Bessel and second kind Hankel functions of the nth order, $\boldsymbol{M}_{nm}^t$ and $\boldsymbol{N}_{nm}^t$ are vector functions defined as follows

$$\boldsymbol{M}_{nm}^t = e^{jm\varphi} \left\{ \frac{jm}{\sin\theta} P_n^m(\cos\theta) \boldsymbol{i}_\theta - \frac{\partial P_n^m(\cos\theta)}{\partial\theta} \boldsymbol{i}_\varphi \right\} \quad (5)$$

$$\boldsymbol{N}_{nm}^t = e^{jm\varphi} \left\{ \frac{\partial P_n^m(\cos\theta)}{\partial\theta} \boldsymbol{i}_\theta + \frac{jm}{\sin\theta} P_n^m(\cos\theta) \boldsymbol{i}_\varphi \right\} \quad (6)$$

and $P_n^m(\cdot)$ is an associated Legendre function [25].

To determine the scattering matrix of the junction, first we enforce the tangential field continuity conditions on the surface $\mathcal{S}$, which take the following form

$$\boldsymbol{E}_t^{\mathrm{I}}(R, \varphi, \theta) = \begin{cases} \boldsymbol{E}_t^{\mathrm{II},i}(R, \varphi, \theta) & \theta \in [\theta_i, \theta_i + \Delta\theta_i] \\ 0 & \text{otherwise} \end{cases} \quad (7)$$

$$\boldsymbol{H}_t^{\mathrm{I}}(R, \varphi, \theta) = \boldsymbol{H}_t^{\mathrm{II},i}(R, \varphi, \theta), \quad \theta \in [\theta_i, \theta_i + \Delta\theta_i] \quad (8)$$

where

$$\boldsymbol{E}_t^{\mathrm{II},i} = E_\varphi^{\mathrm{II},i}(\tilde{\rho}, \varphi, \tilde{z}) \boldsymbol{i}_\varphi + \left(E_\rho^{\mathrm{II},i}(\tilde{\rho}, \varphi, \tilde{z}) \cos\theta - E_z^{\mathrm{II},i}(\tilde{\rho}, \varphi, \tilde{z}) \sin\theta\right) \boldsymbol{i}_\theta \quad (9)$$

$$\boldsymbol{H}_t^{\mathrm{II},i} = H_\varphi^{\mathrm{II},i}(\tilde{\rho}, \varphi, \tilde{z}) \boldsymbol{i}_\varphi + \left(H_\rho^{\mathrm{II},i}(\tilde{\rho}, \varphi, \tilde{z}) \cos\theta - H_z^{\mathrm{II},i}(\tilde{\rho}, \varphi, \tilde{z}) \sin\theta\right) \boldsymbol{i}_\theta \quad (10)$$

$i = \{1, 2\}$, $\tilde{\rho} = R\sin\theta$, $\tilde{z} = R\cos\theta$, $\theta \in [0, \pi]$ and $\varphi \in [0, 2\pi]$. To solve the problem, the vector functions defined by (5) and (6) are

15

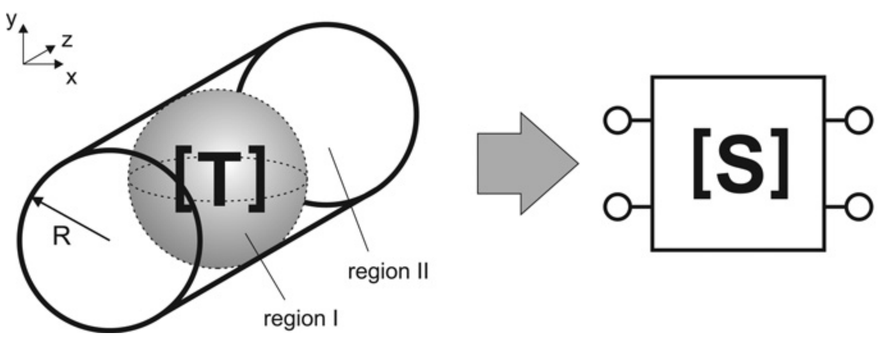

Fig. 2 *Determination of scattering parameters of waveguide junction loaded with ferrite object represented by* ***T****-matrix*

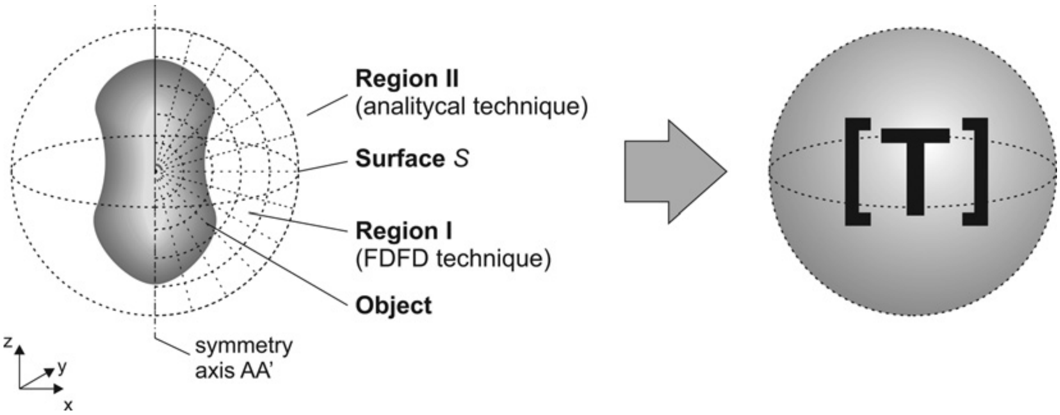

Fig. 3 *Determination of **T**-matrix with the use of hybrid FDFD/MM approach [23]*

used as testing functions for the electric field continuity (7). Simultaneously, the magnetic fields (8) are cross-multiplied by electric field modal vectors of the cylindrical waveguide. The resultant set of linear equations can be written in a matrix form as follows

$$\boldsymbol{M}_t^E \boldsymbol{t} + \boldsymbol{M}_r^E \boldsymbol{r} = \boldsymbol{M}_1^E \boldsymbol{A}_1 + \boldsymbol{M}_2^E \boldsymbol{A}_2 \quad (11)$$

$$\boldsymbol{M}_t^H \boldsymbol{t} + \boldsymbol{M}_r^H \boldsymbol{r} = \boldsymbol{M}_1^H \boldsymbol{A}_1 + \boldsymbol{M}_2^H \boldsymbol{A}_2 \quad (12)$$

For the sake of brevity all matrices are defined in Appendix 1.

The field expansion coefficients in (3) and (4) can be related using transmission matrix $\boldsymbol{T}$ [26, 27] as follows

$$\boldsymbol{A}_2 = \boldsymbol{T}\boldsymbol{A}_1 \quad (13)$$

where $\boldsymbol{A}_1$ is a column vector of known incident field coefficients A_{1nm} (e.g. plane wave or incident waveguide fields) and $\boldsymbol{A}_2$ is a column vector of the unknown scattered field coefficients A_{2nm}. Substituting (13) into (11) and (12) and after some manipulations we obtain

$$\boldsymbol{S} = \left(\boldsymbol{M}_r^H - \boldsymbol{Y}\boldsymbol{M}_r^E\right)^{-1}\left(\boldsymbol{Y}\boldsymbol{M}_t^E - \boldsymbol{M}_t^H\right) \quad (14)$$

where

$$\boldsymbol{Y} = \left(\boldsymbol{M}_1^H + \boldsymbol{T}\boldsymbol{M}_2^H\right)\left(\boldsymbol{M}_1^E + \boldsymbol{T}\boldsymbol{M}_2^E\right)^{-1} \quad (15)$$

Since the $\boldsymbol{T}$-matrix defined for fields in spherical coordinates is known we can easily determine the scattering parameters of the junction. The evaluation of the $\boldsymbol{T}$-matrix for axially symmetrical ferrite posts will be the subject of the following section.

2.2 *T*-matrix

In order to determine the $\boldsymbol{T}$-matrix we utilise the FDFD/MM technique. Since this technique has been thoroughly described in [23] for dielectric/metallic objects and does not involve any special modification for ferrite posts, we will skip its description in this paper (Fig. 3).

The calculated $\boldsymbol{T}$-matrix depends on the geometry and material properties of the object, but not on the excitation. Hence, this approach allows us to limit our consideration to region II, where the scatterer is treated as an effective sphere described by its $\boldsymbol{T}$-matrix. For such an effective sphere the scattered field can be found for any incident wave. The advantage of this approach is that the transmission matrix of the object rotated by any set of Euler angles α, β, γ [28] (see Fig. 4*a*) can be simply derived from the following analytical relation

$$\boldsymbol{T}_{\alpha,\beta,\gamma} = \boldsymbol{D}^{-1}\boldsymbol{T}\boldsymbol{D} \quad (16)$$

where

$$\boldsymbol{D} = \mathrm{diag}\{\boldsymbol{D}_0, \boldsymbol{D}_1, \ldots, \boldsymbol{D}_N\}$$

and $\boldsymbol{D}_n$ are matrices of coefficients defined by the recurrence relations presented in [29].

Moreover, in the analysis of multiple object configurations the iterative scattering procedure (ISP) formulated in spherical coordinates can be used [30, 31] (see Fig. 4*b*). In this procedure, each scatterer is represented by the $\boldsymbol{T}$-matrix. In the ISP, we assume that the incident field on a single post in the Pth iteration is derived from the scattered field from the remaining posts in the previous iteration. At the end of the procedure, the total electric and magnetic fields on surface S_c are obtained. Bearing in mind that the scattered field obtained during the iteration process depends

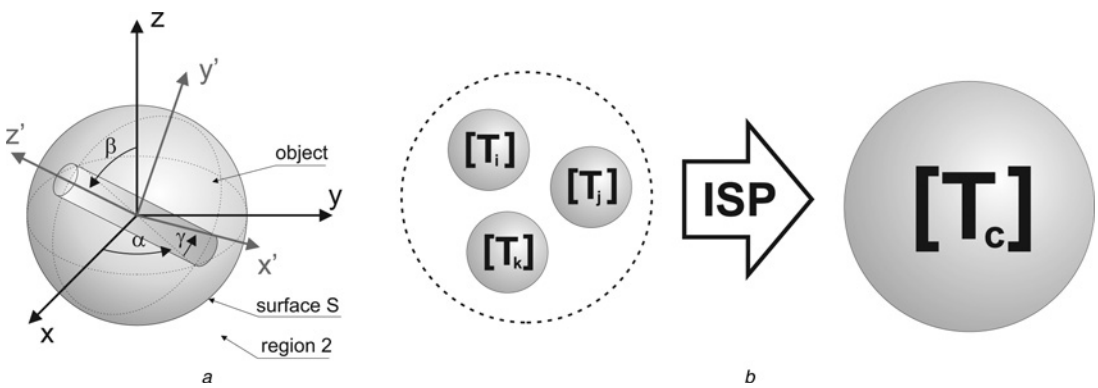

Fig. 4 *Determination of **T**-matrix for arbitrary configuration of objects*

a Post rotation
b Arbitrarily spaced spherical objects

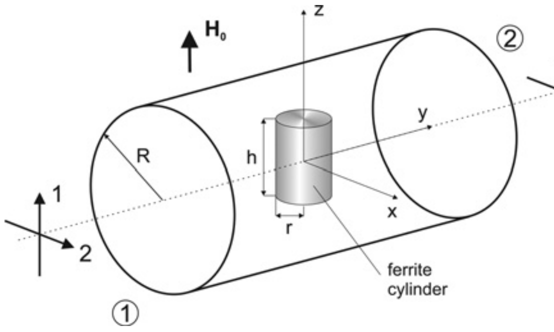

Fig. 5 *Investigated structure of circular waveguide loaded with ferrite cylinder ($R = 10$ mm, $r = 3$ mm, $h = 15$ mm, $\varepsilon_r = 15$, $M_s = 1800$ Gs and $H_i = 0$)*

on the unknown coefficients of the zero-order incident field, the investigated configuration of posts can be described by the total transmission matrix $\boldsymbol{T}_c$. In the above procedure, the fields between each scatterer are translated using an additional theorem of vector spherical harmonics [29]. For particular configurations of objects, the ISP can be sped-up by using the nested ISP [11]. In this approach, at first the effective spheres are evaluated in smaller groups of objects. Next, the total transmission matrix is determined for the group of effective spheres defined in the previous step.

3 Numerical results

The accuracy of the presented approach depends on the number of eigenfunctions used to expand the fields in each region of the structure and the mesh density in the FDFD analysis. Hence, the convergence of the presented approach was investigated and the obtained results are presented in Section 3.1. Next, in Section 3.2, the proposed approach was applied to the analysis of different types of circular waveguide structures loaded with ferrite posts. The calculations of the proposed model were performed in MATLAB environment on Pentium i7-950 3.06 GHz. In order to validate our approach, the obtained results are compared with those calculated using commercial software HFSS [32].

3.1 Convergence

The convergence of the proposed approach was verified for the structure shown in Fig. 5. The structure is composed of circular waveguide containing axially magnetised ferrite cylinder.

Table 1 Absolute value of percentage error $\delta S_{1(1)1(1)}$ of scattering parameters for structure from Fig. 5

N_f	N	Mesh density ($W = I \times J$)			
		20 × 30	40 × 60	80 × 120	160 × 240
2	2	30.8334	27.0733	26.5455	26.2546
	4	14.3776	8.1230	6.9060	6.3367
	6	14.8325	7.9226	6.2160	5.3242
	8	14.7982	7.8944	6.2418	5.3711
4	2	35.7415	31.0444	30.0376	30.9835
	4	15.6678	6.1302	3.0636	2.6405
	6	16.0679	6.1808	2.3696	0.7246
	8	16.0327	6.1573	2.3687	0.6336
6	2	36.0202	29.0379	27.7809	27.3980
	4	16.4116	6.6195	2.8101	1.2758
	6	16.0811	6.1490	2.3238	0.5994
	8	16.0405	6.1331	2.3327	0.5860
8	2	36.6804	28.9989	27.7337	27.3617
	4	16.7355	6.8836	3.0861	1.5078
	6	16.0738	6.1542	2.3388	0.5945
	8	16.0409	6.1331	2.3290	0.5823

In such structures, the field displacement phenomena are observed. Since, the ferrite post is placed at the centre of the waveguide and magnetised along the z-axis, there will be no difference in transmission coefficients ($S_{21} = S_{12}$). Hence, considered structure is reciprocal and only scattering parameters related to port (1) excitation are presented. The scattering parameters of the investigated structure were calculated for different number of eigenfunctions N_f and N in (1)–(4) and different mesh densities. The convergence of the reflection coefficient for TE_{11}^z-mode is presented in Table 1.

The following error criterion was assumed

$$\delta = \frac{||S_{11} - S_{11}^{\text{RA}}||}{||S_{11}^{\text{RA}}||}, \quad \text{where } ||\cdot|| = \sqrt{\int_{f_{\min}}^{f_{\max}} |\cdot|^2 \, \mathrm{d}f}$$

and S^{RA} is frequency-dependent scattering pattern obtained from a Richardson approximation [33]. From the results in Table 1, it can be seen that the percentage error δ decreases with the increasing number of eigenfunctions N_f and N used to expressed the fields in the analysis and the number of mesh densities W. For $N_f = 8$, $N = 6$ and $W = 160 \times 240$ the error is up to 0.59%. The frequency-dependent characteristics of reflection coefficients are presented in Fig. 6 for the chosen number $N = 6$, $N_f = 4$ of eigenfunctions and mesh density $W = 80 \times 120$ and compared with those calculated with the use of commercial software [32]. From the presented results, it

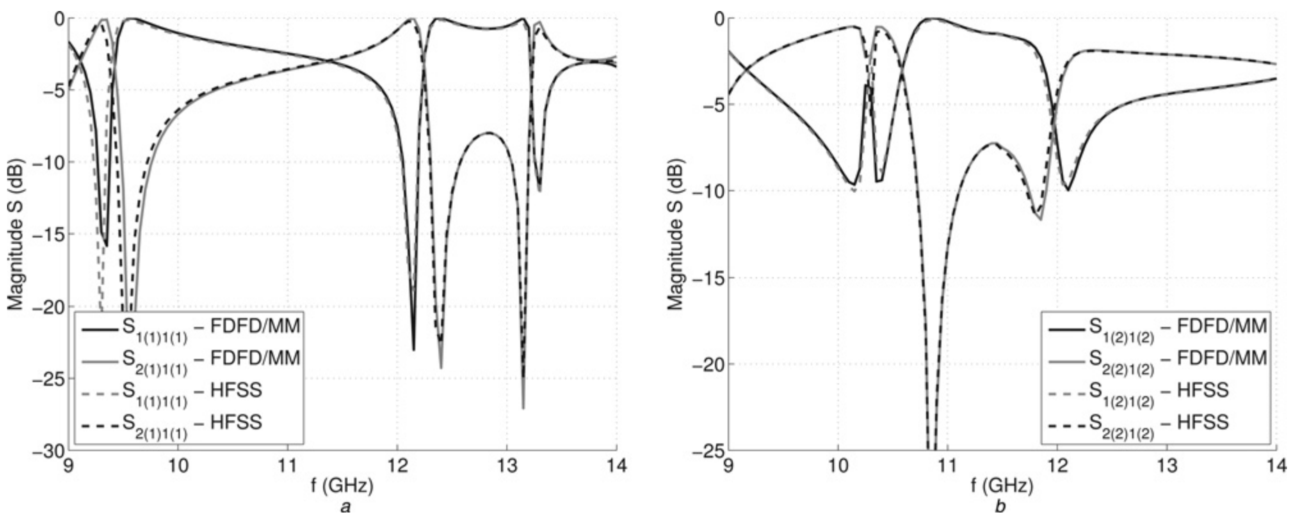

Fig. 6 *Scattering parameters of the structure from Fig. 5 for TE_{11} excitation*

a E-field polarised along the *z*-axis
b E-field polarised along the *x*-axis

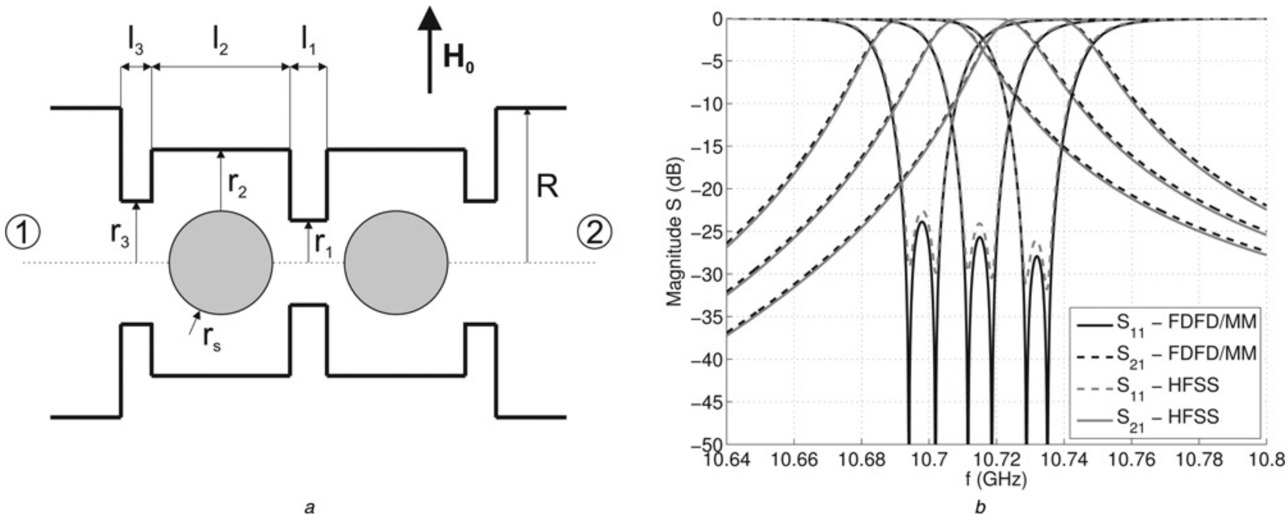

Fig. 7 *Investigated structure of circular waveguide filter loaded with transversally magnetised two ferrite spheres resonators (waveguide housing R = 10 mm, r_1 = 3.79 mm, r_2 = 7.62 mm, r_3 = 4.81 mm, l_1 = 1.16 mm, l_2 = 7.48 mm, l_3 = 1.04 mm, ferrite spheres r_s = 3.42 mm, ε_r = 15 and M_s = 1800 Gs)*

a Schematic view of the structure
b Scattering parameters for H_i = {1, 5, 9} kA/m

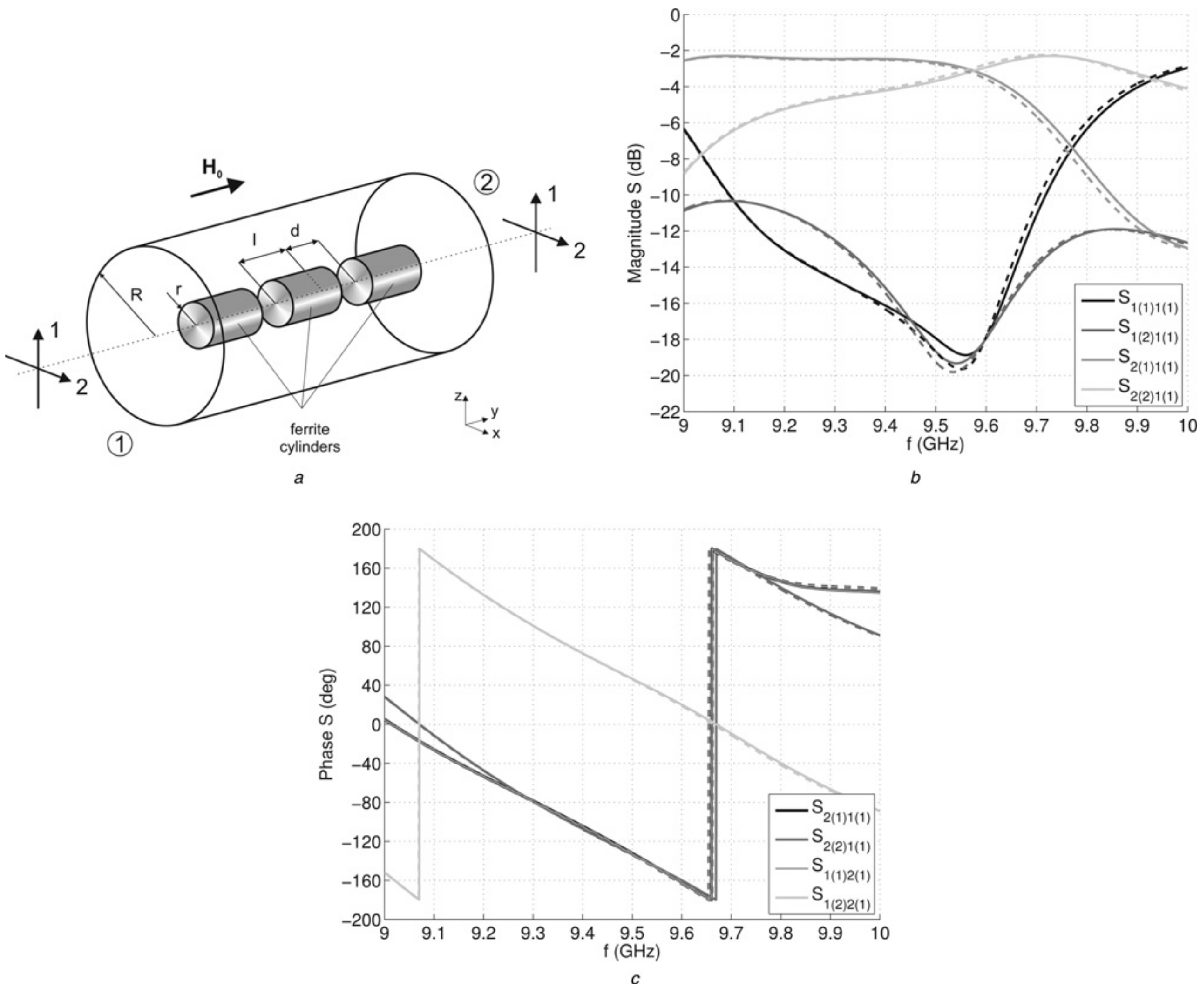

Fig. 8 *Investigated structure of circular waveguide Faraday rotator with longitudinally magnetised three ferrite cylinders (waveguide housing R = 10 mm, ferrite cylinders: r = 2.5 mm, l = 11 mm, ε_r = 15, M_s = 1800 Gs, H_i = 0, spacing of cylinders d = 8 mm)*

a Schematic view of the structure
b Amplitude scattering parameters
c Phase of transmission coefficients – subscript outside brackets denotes port number and subscript inside brackets denotes mode number – solid line: FDFD/MM, dashed line: HFSS

can be noticed that the chosen values of N, N_f and W are enough to obtain satisfactory accuracy compared to the reference results.

The time of analysis for these parameters using proposed approach was about 5.8 s per single frequency point, whereas the calculation time of HFSS with 9432 tetrahedra was about 18 s.

3.2 Applications

In order to validate the proposed approach we applied it to the analysis of two structures presented in Figs. 7*a* and 8*a*. The first analysed structure is a circular waveguide filter composed of two transversely (along the x-axis) magnetised ferrite spheres, presented in Fig. 7*a*.

The scattering parameters of the investigated filter were calculated for TE_{11} mode polarised along the direction of the biasing magnetic field. Three different values of internal magnetic field $H_i = \{1, 5, 9\}$ kA/m (see Fig. 7*b*) were assumed in the analysis. Since, similarly to structure from Fig. 5, the analysed waveguide junction is reciprocal only scattering parameters related to port (1) excitation are presented. From the obtained results, it can be seen that for $H_i = 0$ the filter has an operation bandwidth with a 20 dB reflection coefficient in a frequency range from 10.691 to 10.703 GHz ($\Delta f = 12$ MHz). When the biasing magnetic field is changed, the operation bandwidth of the filter shifts towards higher frequencies, thus allowing for tuning characteristics of the filter. The obtained results are compared with those calculated using commercial software HFSS and good agreement is obtained. The computations using the proposed approach were carried out for $W = 80 \times 120$ mesh cells, $M = 8$ and $N_1 = 8$, $N_2 = 6$, $N_3 = 10$, $N_4 = 4$ for the cavities with radii r_1, r_2, r_3 and r_4, respectively. The analysis time of proposed approach was about 24 s per single frequency point whereas the calculation time of HFSS with 67268 tetrahedra was about 108 s.

The next investigated structure is a cylindrical waveguide loaded with three longitudinally magnetised ferrite cylinders (see Fig. 8*a*). For the considered structure, the scattering parameters were calculated and presented in Fig. 8*b* assuming two orthogonally polarised TE_{11} modes.

From the presented results, it can be noticed that at frequency $f_0 =$ 9.55 GHz the signal is equally divided between two orthogonally polarised TE_{11} output modes, thus allowing to obtain 45° rotation of the electromagnetic field. The phase of the transmission coefficients (see Fig. 8*c*) defined between opposite ports and orthogonal modes depends on the excited port (e.g. $S_{2(2)1(1)} \neq S_{1(1)2(2)}$), which means that the structure is non-reciprocal. This property can be utilised in the realisation of circulators or isolators for wireless communication systems. The obtained results are compared with those obtained from commercial software HFSS. Once again satisfactory agreement is observed between the presented results. The calculations using proposed approach were carried out for $W = 80 \times 120$ mesh cells, $M = 8$ and $N = 8$. The analysis time of proposed approach was about 12 s per single frequency point whereas the calculation time of HFSS with 45029 tetrahedra was about 89 s. For the considered in this section structures the proposed technique was at least about five times faster than commercial software based on FEM.

4 Conclusion

This paper presents a hybrid technique for the analysis of circular waveguide junctions loaded with axially symmetrical ferrite posts. The method is based on the combination of the FDFD technique with MM method. The convergence of the method is verified and discussed. The proposed technique is applied to the analysis of microwave devices such as filter or Faraday rotator. The obtained results are compared to those obtained utilising commercial software, and good agreement is observed. The proposed approach allows us to speed up the analysis in comparison to commercial software, and despite its geometrical limitations seems to be quite attractive approach for the analysis of waveguide junctions loaded with ferrite posts.

5 Acknowledgments

Author thanks Professor J. Mazur from Gdansk University of Technology for his consultation and help during paper preparation. This work was supported in part by the Polish Ministry of Science and Higher Education from sources for science in the years 2012–2013 under Contract IP2011 028271 (decision No. 0282/IP3/2011/71 and in part from the sources of National Science Center under grant decision no. DEC-2013/11/B/ST7/04309.

6 References

1 Yung, E.K.-N., Chen, R.S., Wu, K., Wang, D.X.: 'Analysis and development of millimeter-wave waveguide junction circulator with a ferrite sphere', *IEEE Trans. Microw. Theory Tech.*, 1998, **46**, (11), pp. 1721–1734
2 Wu, H.C., Dou, W.-B.: 'Field structures of waveguide junction circulators with irregular shaped ferrite simulated based on exact treatment', *Prog. Electromagn. Res.*, 2006, **57**, pp. 33–54
3 Kusiek, A., Marynowski, W., Mazur, J.: 'Investigations of the circulation effects in the structure using ferrite coupled slot-line section', *Microw. Opt. Technol. Lett.*, 2007, **49**, (3), pp. 692–696
4 O'Neil, B.K., Young, J.L.: 'Experimental investigation of a self-biased microstrip circulator', *IEEE Trans. Microw. Theory Tech.*, 2009, **57**, (7), pp. 1669–1674
5 Seewald, C.K., Bray, J.R.: 'Ferrite-filled antisymmetrically biased rectangular waveguide isolator using magnetostatic surface wave modes', *IEEE Trans. Microw. Theory Tech.*, 2010, **58**, (6), pp. 1493–1501
6 Fesharaki, F., Akyel, C., Wu, K.: 'Broadband substrate integrated waveguide edge-guided mode isolator', *Electron. Lett.*, 2013, **49**, (4), pp. 269–271
7 Hui, W.W.G., Bell, J.M., Iskander, M.F., Lee, J.J.: 'Low-cost microstrip-line-based ferrite phase shifter design for phased array antenna applications', *IEEE Trans. Antennas Propag.*, 2007, **6**, pp. 86–89
8 Sorensen, R.K., Iskander, M.F., Lee, J.J.: 'Low-cost nonplanar microstrip-line ferrite phase shifter utilizing circular polarization', *IEEE Microw. Theory Wirel. Compon. Lett.*, 2004, **14**, (1), pp. 25–27
9 Baden-Fuller, A.J.: 'Ferrites at microwave frequencies' (Peter Peregrinus Ltd., UK, 1987)
10 Chen, R.S., Yung, E.K.-N.: 'An efficient method to analyze the h-plane waveguide junction circulator with a ferrite sphere', *IEEE Trans. Microw. Theory Tech.*, 2001, **49**, (5), pp. 928–937
11 Polewski, M., Mazur, J.: 'Scattering by an array of conducting lossy dielectric, ferrite and pseudochiral cylinders', *Prog. Electromagn. Res.*, 2002, pp. 283–310
12 Geng, Y.-L.: 'Scattering of a plane wave by an anisotropic ferrite-coated conducting sphere', *IET Microw. Antennas Propag.*, 2008, **2**, (2), pp. 158–162
13 Polewski, M., Lech, R., Mazur, J.: 'Oblique plane wave scattering by an array of dielectric and metamaterial cylinders'. 15th Int. Conf. on Microwaves, Radar and Wireless Communications, 2004, MIKON-2004, May 2004, vol. 2, pp. 409–412
14 Yung, E.K.-N., Chen, R.S., Wang, Y., Wu, K.: 'Fdtd analysis of em wave circulated by a magnetised ferrite body of arbitrary shape', *IEE Proc., Microw. Antennas Propag.*, 1998, **145**, (6), pp. 433–440
15 Gwarek, W.K., Moryc, A.: 'An alternative approach to FD-TD analysis of magnetized ferrites', *IEEE Microw. Theory Wirel. Compon. Lett.*, 2004, **14**, (7), pp. 331–333
16 Pereda, J.A., Grande, A., Gonzalez, O., Vegas, A.: 'Some numerical aspects of an extension of the FDTD method to incorporate magnetized ferrites'. Workshop on Computational Electromagnetics in Time-Domain, 2007, CEM-TD 2007, October 2007, pp. 1–4
17 Zhou, L., Davis, L.E.: 'Finite-element method with edge elements for waveguides loaded with ferrite magnetized in arbitrary direction', *IEEE Trans. Microw. Theory Techn.*, 1996, **44**, (6), pp. 809–815
18 Madanifar, K.A., Kamyab, M.: 'A comparative FDTD analysis of magnetized ferrites'. Asia-Pacific Conf. on Applied Electromagnetics, 2007, APACE 2007, December 2007, pp. 1–4
19 Epp, L.W., Hoppe, D.J., Chinn, G.C.: 'Scattering from ferrite bodies of revolution using a hybrid approach', *IEEE Microw. Guided Wave Lett.*, 1995, **5**, (4), pp. 111–113
20 Polycarpou, A.C., Balanis, C.A.: 'Analysis of ferrite loaded cavity backed slot antennas using a hybrid fem/mom approach'. IEEE Antennas and Propagation Society Int. Symp., July 1997, vol. 2, pp. 652–655
21 Wu, H.C., Dou, W.-B.: 'Field structures of waveguide junction circulators with irregular shaped ferrite simulated based on exact treatment', *Prog. Electromagn. Res.*, 1995, **57**, pp. 33–54
22 Kusiek, A., Lech, R., Mazur, J.: 'A new hybrid method for analysis of scattering from arbitrary configuration of cylindrical objects', *IEEE Trans. Antennas Propag.*, 2008, **56**, (6), pp. 1725–1733
23 Kusiek, A., Mazur, J.: 'Hybrid finite-difference/mode-matching method for analysis of scattering from arbitrary configuration of rotationally-symmetrical posts', *Prog. Electromagn. Res.*, 2010, **110**, pp. 23–24
24 Gardiol, F.E.: 'Introduction to microwaves' (Artech House, USA, 1984)
25 Stratton, J.A.: 'Electromagnetic theory' (Wiley, USA, 2007)
26 Waterman, P.C.: 'Matrix formulation of electromagnetic scatterings', *Proc. IEEE*, 1965, **53**, pp. 805–811
27 Peterson, B., Strom, S.: 'T matrix for electromagnetic scattering from an arbitrary number of scatterers and representation of e(3)', *Phys. Rev. D*, 1973, **8**, pp. 3661–3678

28 Tsang, L., Kong, J.A., Ding, K.-H.: 'Scattering of electromagnetic waves: theories and applications' (John Wiley and Sons, Inc., New York, 2000)
29 Mackowski, D.W.: 'Analysis of radiative scattering for multiple sphere configurations', *Proc. R. Soc. A, Math. Phys. Sci.*, 1991, **433**, (1889), pp. 599–614
30 Hamid, A.-K., Ciric, I.R., Hamid, M.: 'Iterative solution of the scattering by an arbitrary configuration of conducting or dielectric spheres', *IEE Proc. H Microw. Antennas Propag.*, 1991, **138**, (6), pp. 565–572
31 Defos du Rau, M., Pessan, F., Vigneras-Lefebvre, V., Parneix, J.P.: 'Multiple scattering in heterogeneous media with spherical inclusions'. Third Int. Conf. on Computation in Electromagnetics, (Conf. Publ. No. 420), April 1996, pp. 387–392
32 High Frequency Structure Simulator (HFSS). http://www.ansoft.com/
33 Dahlquist, G., Bjorck, A.: 'Numerical methods' (Prentice-Hall, 1974)

7 Appendix

In (11) and (12), matrices of electric $\boldsymbol{M}^E_{t(r)}$, $\boldsymbol{M}^E_{1(2)}$ and magnetic fields $\boldsymbol{M}^H_{t(r)}$, $\boldsymbol{M}^H_{1(2)}$ are block diagonal matrices with respect to m parameter and take a the following form

$$\boldsymbol{M}^E_{t(r),m} = \begin{bmatrix} \boldsymbol{ME}^{M,\mathrm{TM}}_{t(r),m} & \boldsymbol{ME}^{M,\mathrm{TE}}_{t(r),m} \\ \boldsymbol{ME}^{N,\mathrm{TM}}_{t(r),m} & \boldsymbol{ME}^{N,\mathrm{TE}}_{t(r),m} \end{bmatrix} \tag{17}$$

where

$$\left[\boldsymbol{ME}^{M,\nu}_{t(r),m}\right]_{nl} = \iint_S \boldsymbol{E}^{\nu}_{t(r),lm} \cdot \boldsymbol{M}^t_{n(-m)} \sin\theta \,\mathrm{d}\theta\,\mathrm{d}\varphi$$

$$\left[\boldsymbol{ME}^{N,\nu}_{t(r),m}\right]_{nl} = \iint_S \boldsymbol{E}^{\nu}_{t(r),lm} \cdot \boldsymbol{N}^t_{n(-m)} \sin\theta \,\mathrm{d}\theta\,\mathrm{d}\varphi$$

and $\nu = \{\mathrm{TM}, \mathrm{TE}\}$, $\boldsymbol{E}^{\nu}_{t(r),lm}$ denotes the lmth term of the transmitted (t) and reflected (r) tangential electric field defined on spherical surface $\mathcal{S}$ in region II

$$\boldsymbol{M}^E_{1(2),m} = \begin{bmatrix} \boldsymbol{ME}^{M,M}_{1(2),m} & 0 \\ 0 & \boldsymbol{ME}^{N,N}_{1(2),m} \end{bmatrix} \tag{18}$$

where

$$\left[\boldsymbol{ME}^{M,M}_{1(2),m}\right]_{nn} = (-1)^m \frac{2n(n+1)}{2n+1} z_n^{1(2)}(k_0 r)$$

$$\left[\boldsymbol{ME}^{N,N}_{1(2),m}\right]_{nn} = (-1)^m \frac{2n(n+1)}{2n+1} \frac{\partial r z_n^{1(2)}(k_0 r)}{k_0 r \partial r}$$

$$\boldsymbol{M}^H_{t(r),m} = \begin{bmatrix} \boldsymbol{MH}^{\mathrm{TM,TM}}_{t(r),m} & \boldsymbol{MH}^{\mathrm{TM,TE}}_{t(r),m} \\ \boldsymbol{MH}^{\mathrm{TE,TM}}_{t(r),m} & \boldsymbol{MH}^{\mathrm{TE,TE}}_{t(r),m} \end{bmatrix} \tag{19}$$

where

$$\left[\boldsymbol{MH}^{\alpha,\nu}_{t(r),m}\right]_{nl} = \iint_S \boldsymbol{H}^{\alpha,\nu}_{t(r),lm} \times \left(\boldsymbol{E}^{\alpha,\nu}_{t(r),lm}\right)^* \sin\theta \,\mathrm{d}\theta\,\mathrm{d}\varphi$$

$$\boldsymbol{M}^H_{1(2),m} = \begin{bmatrix} \boldsymbol{MH}^{\mathrm{TM},N}_{1(2),m} & \boldsymbol{MH}^{\mathrm{TM},M}_{1(2),m} \\ \boldsymbol{MH}^{\mathrm{TE},N}_{1(2),m} & \boldsymbol{MH}^{\mathrm{TE},M}_{1(2),m} \end{bmatrix} \tag{20}$$

where

$$\left[\boldsymbol{MH}^{\nu,N}_{1(2),m}\right]_{nl} = \iint_S \boldsymbol{N}^t_{nm} \times \left(\boldsymbol{E}^{\mathrm{TM}}_{r,lm}\right)^* \sin\theta \,\mathrm{d}\theta\,\mathrm{d}\varphi$$

$$\left[\boldsymbol{MH}^{\nu,M}_{1(2),m}\right]_{nl} = \iint_S \boldsymbol{M}^t_{nm} \times \left(\boldsymbol{E}^{\mathrm{TE}}_{r,lm}\right)^* \sin\theta \,\mathrm{d}\theta\,\mathrm{d}\varphi$$

The column vector of transmission coefficients $\boldsymbol{t}$ takes the form $\boldsymbol{t} = \left[\boldsymbol{t}^{\mathrm{TM}}_{-M}, \ldots, \boldsymbol{t}^{\mathrm{TM}}_{M}, \boldsymbol{t}^{\mathrm{TE}}_{-M}, \ldots, \boldsymbol{t}^{\mathrm{TE}}_{M}\right]^{\mathrm{T}}$ and $\boldsymbol{t}^{(\cdot)}_m = \left[t^{(\cdot)}_{m0}, t^{(\cdot)}_{m1}, \ldots, t^{(\cdot)}_{mN}\right]$. The column vector of reflection coefficients $\boldsymbol{r}$ is defined analogously.